Nanomedicine

Drug loaded liposome capped mesoporous core-shell magnetic nanoparticles for cellular toxicity study

Journal:	*Nanomedicine*
Manuscript ID	NNM-2016-0248.R2
Manuscript Type:	Research Article
Keywords:	Controlled drug release, Liposomes, Nanotoxicity

Drug loaded liposome capped mesoporous core-shell magnetic nanoparticles for cellular toxicity study

Maneea Eizadi Sharifabad[1,2], Tim Mercer[2] and Tapas Sen[1,2*]

*corresponding authors details

[1] Nano-biomaterials Research Group (www.senlabs.org)
[2] School of Physical Sciences & Computing
Centre of Materials Sciences,
University of Central Lancashire,
Preston, PR1 2HE, United Kingdom
Tel: +44 1772894371
Email: tsen@uclan.ac.uk

Keywords: Core-shell, Superparamagnetic Iron Oxide Nanoparticles (SPIONs), Mesoporous Silica, Drug Delivery, Doxorubicin, Alternating Magnetic Field (AMF), Magnetic Hyperthermia

ABSTRACT

Liposome-capped core-shell mesoporous silica coated superparamagnetic iron oxide nanoparticles called “magnetic protocells“ were prepared as novel nanocomposites and used for loading anticancer drug doxorubicin (DOX) for celluar toxicity study. Cytotoxicity of the magnetic protocells with or without DOX was tested *in vitro* on commercial MCF7 and U87 cell lines under Alternative Magnetic Field (AMF). MCF 7 cell line treated with the DOX-loaded nanoparticles under AMF exhibited nearly 20% lower survival rate after 24 hrs compared to cells treated with free DOX and similarly it was around 24% when applied to U87. The results indicate that the magnetic protocells could be useful for future cancer treatment *in vivo* by the combination of targeted drug delivery and magnetic hyperthermia.

Keywords: Core-shell, Superparamagnetic Iron Oxide Nanoparticles (SPIONs), Mesoporous Silica, Doxorubicin, Alternating Magnetic Field (AMF), Magnetic Hyperthermia, cytotoxicity

Introduction

Despite advances in diagnostic procedures and treatments, the overall survival rate from cancer has not improved substantially over the past 30 years [1]. One promising development is the encapsulation of toxic cancer chemotherapeutic agents within biocompatible nanocomposite materials. Encapsulating the drugs within nanoparticles with stimuli triggered drug release can overcome the difficulties presented by the 'free' drug via improving the solubility, stability, and increased selectivity towards targeted tissues, which results in decreased toxicity toward healthy cells and reduces the necessary drug dosage to eliminate malignant cells [2].

Here the synthesis of novel magnetic mesoporous nanoparticles capped with lipid bilayers (magnetic protocells) is reported. Magnetic protocells combine the properties of superparamagnetic iron oxide nanoparticles (SPIONs), mesoporous silica nanoparticles (MSN), and liposomes - realizing the synergistic effects of hyperthermia and chemotherapy. SPIONs have shown great potential as theranostic systems in nanomedicine since they can be used as both magnetic resonance imaging (MRI) contrast agents [3], and hyperthermia agents [4]. MSN's are widely studied for drug delivery applications due to their biocompatibility, high surface area, tunable mesopore structure, and modifiable surface [2, 5-10]. Recently, the feasibility of the mesoporous silica based nanoparticles in order to deliver an extensive range of drugs and therapeutic agents has been widely explored [11-14]. Typically the drug / cargo is loaded in mesoporous silica nanoparticles through simple electrostatic interactions or physical absorption [15-17]. The release profiles of mesoporous nanoparticles can be partly adjusted by altering the pore size and pore surface chemistry [18]. However, without proper pore capping drugs loaded into the accessible pores through electrostatic interactions or physical adsorption, could easily leach out into the blood stream and premature drug release is inevitable [18]. Additionally mesoporous nanoparticles low dispersibility and aggregation under physiological conditions, and their nonspecific binding in protein containing solutions limit their applications in biomedicine [19]. On the other hand, liposomes are one of the most broadly studied nanocarriers due to their biocompatibility and biodegradability [20]. Capping mesoporous nanoparticles with liposomes should reduce the premature drug release and improve the circulation time of mesoporous

nanoparticles. Furthermore the MSN supports improve the bilayer stability and provide higher drug loading content than same size liposomes [21]. When drug-loaded nanoparticles are placed in alternating magnetic fields, stirring and hysteresis effects of the magnetic core of the nanoparticles generates localized heat which affects the thermosensitive liposomes layer releasing the encapsulated drug. DOX loading and liposome capping of the mesoporous magnetic nanocomposites are illustrated in Scheme 1. In this context an alternate method has recently been published by Podaru *et al* [22] using pulsed Magnetic Field induced fast drug release from magneto liposomes without any mesoporous shell *via* ultrasound generation.

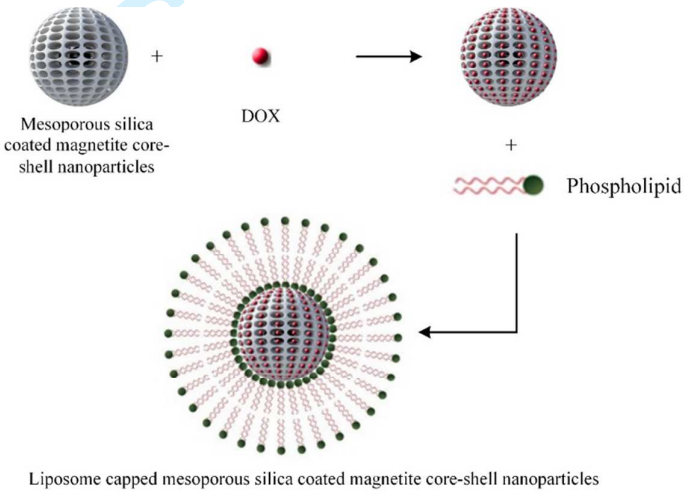

Scheme 1 *The process of DOX loading of the liposome capped silica magnetite core-shell nanoparticles*

Materials and methods

- Materials and reagents

Chemical reagents employed for synthesis of materials were purchased from Sigma-Aldrich, UK and used without further purification. Doxorubicin hydrochloride (DOX) was purchased from Cayman Chemical. PrestoBlue Cell Viability reagent was purchased from Invitrogen. Eagle's Minimum Essential Medium (EMEM), Fetal bovine serum (FBS), L-glutamine, Non Essential Amino Acids (NEAA), and Sodium

Pyruvate were purchased from Lonza. U87 and MCF7 commercial cell lines were kindly provided by UCLan tissue culture lab.

- Preparation of DOX loaded magnetic protocells

Protocells were synthesized by coating liposomes over magnetic mesoporous nanoparticles. Natural phospholipid (soybean phosphatidylcholine, SPC) was used to prepare the lipid bilayer. The use of SPC instead of the commonly used synthetic phospholipids such as dioleoyl phosphatidylethanolamine (DOPE) and dipalmitoyl phosphatidylcholine (DPPC) leads to much lower cost and better serum stability [2]. Cholesterol was added to phospholipids to increase the lipid packing density and decrease the drug diffusion across the bilayer [23]. Liposomes were prepared by hydration of lipid films. The mesoporous nanoparticles were prepared using the modified Stober method with cetyl triethyl ammomium bromide (CTAB) as the template for mesoporous structure following our previously reported method [24]. Mesoporous silica coated magnetic nanoparticles (10 mg) were washed with 5mL of PBS buffer (×3) followed by immersion in DOX solution (10 mL, 0.18 mg/mL) in an incubator set at 18^{o} C . After 4 hours of immersion, as-prepared liposome solution (2.5 mL, 4 mg/mL) following our earlier published protocol [25, 26] was added to the drug-nanoparticle mixture and underwent ultrasounication using a titanium horn sonicator in order to obtain a homogeneous solution. During the ultrasonication, the mixture was placed in an ice bath to protect it from overheating and to obtain a homogeneous solution. The mixture was then placed in an incubator at 18°C and stirred by end over end rotation for a further 48 hours. The drug loading profile was evaluated at different time intervals by measuring UV absorption at λ_{485nm}. The drug loaded nanoparticles were collected and stored under freeze dried condition for the drug release and cytotoxicity studies.

The drug loading and drug loading efficiency (DLE) were assessed after incubation of the drug loaded mesoporous core-shell nanoparticles with liposome mixture. To quantify the amount of the drug loaded into the nanoparticles, the magnetic protocells were separated by centrifuge and the UV absorbance of the supernatant

was measured at λ_{485} nm. The concentration of DOX was calculated using a previously established standard curve of DOX in PBS buffer.

- DOX release methodology

DOX-loaded freeze-dried nanocomposites were suspended in 3 mL of PBS buffer (pH 7.4), covered with aluminum foil and placed in an incubator at 37^{o}C which is equivalent to body temperature and stirred under end over end rotation (40 rpm) for up to 48 hours. The DOX concentrations at different time intervals were calculated by measuring the UV absorbance at λ_{485} nm and comparing it with the pre-established standard curve of DOX prepared in the same solution.

- Methodology for hyperthermia under AMF

Magnetic heating was performed using a commercial AC field applicator, DM2, with a system controller DM100 by nB nanoscale Biomagnetics, Spain. All the experiments were performed at a frequency of 406 kHz and the temperature was monitored using a fibre optic temperature sensor (Measuring range: -10ºC to 120 ºC with precision: ±0.2 ºC) and controlled by adjusting the magnetic field strength. The maximum field strength was 200G. The accepted frequency using magnetic hyperthermia is reported to be between 100 kHz to 1 MHz [27]. System embedded software, MaNIaC, was used to control the experiments and collect the data. The magnetic induced heating of the nanocomposites under AMF was evaluated by dispersing 10 mg of the nanoparticles in 1 mL of DI water which was then placed in the AC field with an overhead rotator (40 rpm) for 45 minutes. The temperature was set at 43°C which is sufficient for classical hyperthermia treatment for cancer therapy [28]. Experiments using commercial Cell-lines were performed by placing the T-25 flask directly in the DM2 field applicator.

- Cytotoxicity study

Two commercial cell lines such as human breast adenocarcinoma (MCF7) and glioblastoma (U87) were used in this study. ATCC (American type culture collection) recommended growth medium (Eagle's Minimum Essential Medium (EMEM)+10% (v/v) Fetal Bovine Serum (FBS)) with the addition of Non-Essential Amino Acids Solution (NEAA, 1%), Sodium Pyruvate (1%), Penicillin Streptomycin (Pen Strep, 1%) and L-Glutamine (1%) were used for both cell lines. The seeding densities of MCF7 and U87 cells were about 5×10^4 cells/cm^2 and 4×10^4 cells/cm^2 in T-75 flask containing 10 mL of the growth medium as recommended by ATCC [29, 30].

Cytotoxicity assessments were performed using PrestoBlue reagent according to the manufacturer's protocol. Cells were harvested at the logarithmic growth phase and seeded in 96 well plates. Cells were maintained in complete growth medium for 24 hours at 37°C in a humidified atmosphere with 5% CO_2. After 24 hours the medium was removed and replaced with 100 µL of media containing different concentrations of a synthesised nanomaterials. Subsequently, the cell viability was measured at different periods of up to 72 hours using PrestoBlue assay. To perform the assay, the medium was removed and replaced by 100 µL of fresh growth media and 10 µL of PrestoBlue reagent. The plates were covered with aluminium foil and incubated for 30 minutes. The fluorescence was measured using excitation at 535 nm and emission at 612 nm using the Tecan Genius Pro Plate Reader.

We have initially tested the effect of nanoparticles concentration on PestoBlue assay and it was found that the concentrations of nanoparticles which were used in our experiments were below the interference limit. We have previously reported [26, 31] a dose dependent cytotoxicity study and in our current study, we have used an optimum concentration of nanoparticles which is non-toxic without the presence of DOX and didn't interfere with the fluorescence measurement during PestoBlue assay.

IC50 of DOX-loaded materials were calculated from the viability tests performed using different concentration of DOX-loaded nanoparticles and compared with the IC50 obtained for free DOX.

- Effect of AMF on Cell Viability

Cells were collected at 70% confluence and seeded into T-25 flasks and incubated with 5 mL of growth media at 37°C ± 1°C in 5% CO_2 for 2 days. After 2 days the medium was removed and replaced with different concentrations (0.25, 0.5, 0.75, and 1 mg/ml) of magnetic protocells, core magnetite and mesoporous silica coated magnetic nanoparticles. Cells were incubated with the nanoparticles for further 24 hours. After 24 hours, the media containing nanoparticles was removed and replaced with fresh media. Cells were then exposed to an AMF for 45 minutes whilst measuring the medium temperature (the field strength was adjusted to maintain the temperature at 43°C). After that, cells were placed back in the incubator at 37°C ± 1°C in 5% CO_2. The cell viability was measured 2 hours and 24 hours post magnetic hyperthermia treatment using PrestoBlue assay.

- Statistical Analysis

All results are reported as the mean (average) of at least three independent experiments with error bar presenting the standard deviation (SD). In case of the tissue culture experiments, each experiment was repeated at least 3 times and measured using no less than six wells per experiment. Statistical analyses were performed by t-tests where P values less than 0.05 were considered to be statistically significant.

- Size measurements

Dynamic light scattering (DLS) experiments were performed to estimate the particles size using a Zetasizer Nano, Malvern Instruments, UK at 23°C. Nanoparticles were suspended in water at a dilute concentration, consequently, 1 mL of the nanoparticle suspensions were placed in a 12 mm (OD) square polystyrene cuvettes for measurements.

- Stability measurements

A built in-house Scanning Column Magnetometer (SCM) was used to measure the concentration profile of a sample column of magnetic dispersion over its height. The SCM operates at a sample-free frequency of 1 MHz and as it scans the dispersion

this causes a shift in the frequency that is directly proportional to the concentration of magnetic particles at that height. Full details of the technique are given elsewhere [32], but by repeating this measurement on each sample at different times a series of concentration profiles can be generated in order to observe the stability of the magnetic suspensions. The samples for the SCM were prepared by sonication of the magnetic suspension using a titanium horn sonicator for 4 minutes followed by placing up to 10 mL of the suspension into the SCM column tubes.

- Specific absorption rate (SAR) values of nanoparticles

The nanoparticles efficiency to generate heat from the magnetic coupling between magnetic moment of nanoparticles and the applied alternate magnetic field could be assessed from specific absorption rate (SAR) calculations. SAR values of core iron oxide nanoparticles, mesoporous silica coated iron oxide nanoparticles, liposome capped mesoporous silica coated iron oxide nanoparticles were calculated to be 176.5, 10.8 and 1.3 W/g from thermal measurement data under AMF.

Results and discussion

- Characterisation of nanoparticles

In a previous report [25] we showed that liposome capped magnetic nanoparticles (Magnetoliposomes or protocells) are stable over a long period (30 days). In the present study liposomes were used to cap the silica mesopores and improve the stability of the magnetic protocells in suspension. The stability of the un-capped mesoporous silica coated magnetic nanoparticles and liposome capped magnetic mesoporous silica nanoparticles (protocells) are presented in Figure 1. The SCM plot for uncapped nanoparticles of part (a) shows a clear change in material concentration over the column height with time. At 40 minutes, a peak was observed in the SCM plot corresponding to the material build-up at the bottom of the column. This could be attributed to the increased magnetic susceptibility at the end of the column as a result of the higher concentration of magnetic particles at this point. It was observed that the peak intensity increased with time indicating an increase in the packing fraction of the magnetic nanomaterials settled at the end of the column. The consistently reducing particle concentration observed across all of the upper

layers in part (a), that occurs whilst a top layer step is maintained at the original (time-zero) column height, is indicative of Stokes-like sedimentation; where particles are free to settle in any given system at a rate determined by their size [32]. There are no obvious changes in the SCM profiles of the magnetic protocells (part b of Figure 1Figure 1) over a period of 4 hours. This indicates that the material was stable over the measurement period, there being no sedimentation in the column. The results shows that liposome coating of the silica coated magnetic nanoparticles effectively increases the stability of the silica coated nanoparticles which is crucial in regards to storage ability and their application in drug delivery.

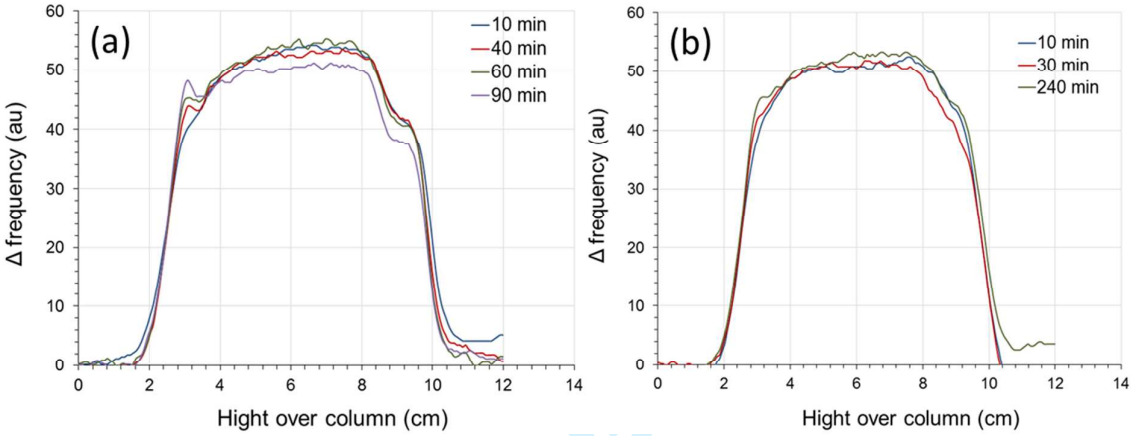

Figure 1. SCM profiles of (a) mesoporous silica coated magnetite nanoparticles and (b) liposome capped *mesoporous silica coated magnetite* nanoparticles showing the frequency shift (change in magnetic particle volume concentration) as a function of dispersion column height.

The hydrodynamic number average size distributions of the protocells before drug loading is presented in Figure 2a. The average hydrodynamic diameter of the particles was determined to be 113 nm with a polydispersity (PDI) index of 0.32. The TEM images of the mesoporous silica coated magnetic nanoparticles without liposome capping shows an average size of around 80 nm (Figure 2b) which can indirectly provide an estimate of the thickness of lipid bilayer in the order of around 16 nm.

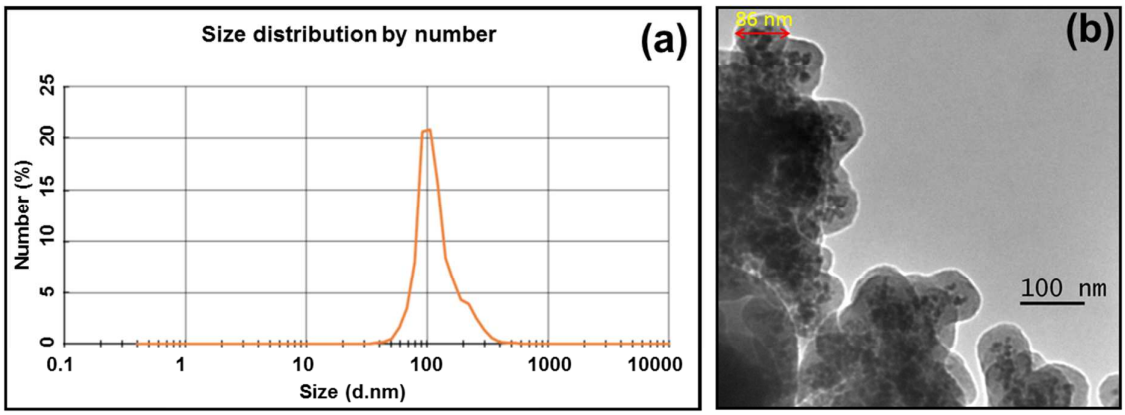

Figure 2. DLS size distribution profile of magnetic *protocells (A); TEM image of mesopoorus silica coated magnetic nanoparticles (B).*

- Drug loading and release

The DOX loading content was calculated to be 59 µg / mg of protocells with a drug loading efficiency (DLE) value of 65.8%. These results indicate that the liposome capped mesoporous silica coated superparamagnetic iron oxide nanoparticles called “protocells” were capable of effectively encapsulating a large amount of DOX molecules and this may be due to the large surface area of the mesoporous silica shells.

DOX release studies from uncapped mesoporous silica coated magnetic nanoparticles and protocells were performed *in vitro* at body temperature (37° C) in physiological pH 7.4 and in an acidic pH of 5.5 as shown in Figure 3 followed by in the presence of AMF (43^{o} C) as presented in Figure 4. Drug release profiles, at pH 7.4 showed that no initial burst release of DOX was observed from magnetic protocells and this could be due to the liposome capping of silica mesopores. Indeed, after liposome capping, DOX release at physiological pH was reduced by 53% compared to uncapped mesoporous silica coated magnetic nanoparticles.

As evident from Figure 3, DOX release ratio was higher in the acidic pH condition compared to the physiological pH condition both for capped (protocells) and uncapped nanoparticles. The total drug release at pH 5.5 and pH 7.4 reached 40.23% and 23.2% for uncapped nanoparticles and 21.9% and 12.89% for capped nanoparticles respectively. It was clear that DOX was released more readily at the

lysosomal pH condition rather than at the physiological blood plasma pH condition. Similar trends of drug release from mesoporous silica have been observed by other groups [12, 15, 33-35]. It is suggested that the increased DOX release from protocells at acidic pH could be due to disruption of the lipid bilayer caused by acidification enabling DOX to diffuse out from the nanocomposites [21].

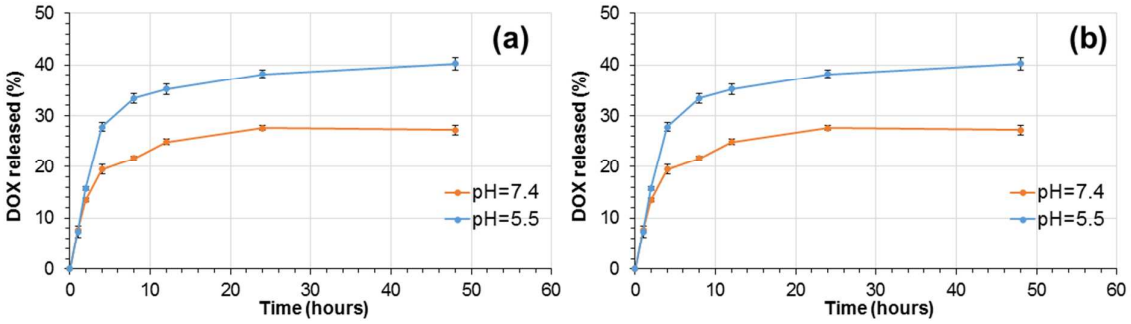

Figure 3. Cumulative doxorubicin release (%) profile from (a) magnetic mesoporous nanoparticles and (b) protocells. The drug release profiles were investigated at pH=7.5 and pH=5.5 at 37°C.

DOX release was studied under AMF to investigate the DOX release from the protocells and evaluated their feasibility for use in simultaneous magnetic hyperthermia and drug delivery for cancer treatment. The results are illustrated in Figure 4. As presented in Figure 4-a, the protocells were able to produce sufficient heat for hyperthermia treatment for cancer therapy.

As shown in Figure 4, only slight change in drug release was observed under elevated temperature both in the incubator and under an AC field. A slow but linear increase in DOX release with time (Figure 4b) at 43^{o}C can be favorable for drug delivery application without affecting the structure of the capped liposomes.

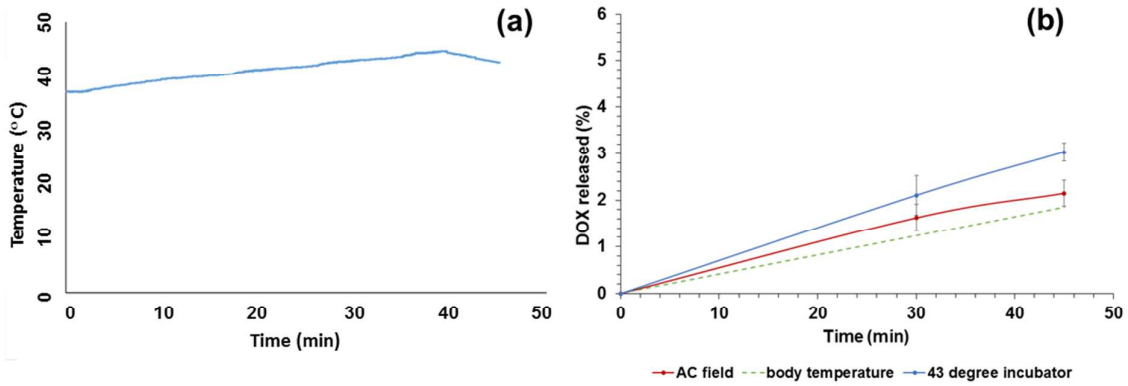

Figure 4. (a) Magnetic heating profile of protocells with the concentration of 10 mg/mL in a variable magnetic field with maximum strength of 200 Gauss and frequency of 406 kHz. The field was adjusted in the way to keep the temperature at 43°C and (b) Heat triggered DOX release profile of protocells.

In Vitro Cytotoxicity of the Nanocomposites

MCF7 and U87 cell lines were treated with bare nanoparticles, uncapped mesoporous silica coated nanoparticles and protocells with different concentration of 0.25 mg/mL, 0.5 mg/mL, 0.75 mg/mL and 1 mg/mL and the cell viability were measured after 3, 24, 48 and 72 hours. The cytotoxicity of the nanoparticles after 72 hours are shown in Figure 5. The results are shown as cell viability percentage compared to untreated control cells. The data demonstrated that only bare magnetite nanoparticles induced toxicity in the low dosage of 0.25 mg/mL. It was shown that the biocompatibility of the magnetite nanoparticles were significantly improved by silica coating. Mesoporous silica coated nanoparticles showed good biocompatibility against both cell lines, however they exhibited cytotoxicity at high dose or after long incubation period. The toxicity was observed to be cell dependent which is in agreement with literature [36]. The mesoporous nanoparticles exhibited relatively higher toxicity toward U87 cell lines than MCF7 cells. The different cytotoxicity induced by nanomaterials is suggested to be due to the differences in their surface composition.

As seen in the figures, it was established that the protocells exhibited relatively greater biocompatibility than uncoated silica nanoparticles against both cell lines. Protocells were biocompatible and exhibited very limited toxicity against both cell

lines. The biocompatibility of the mesoporous nanoparticles were clearly improved by liposome capping of the mesoporous silica coated magnetic nanoparticles.

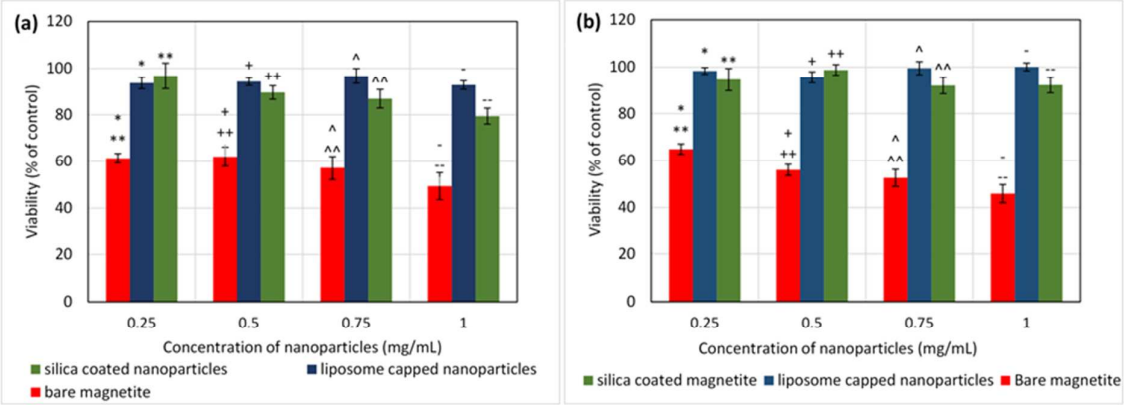

Figure 5. Cytotoxicity of silica coated magnetite, liposome capped silica coated nanoparticles (magnetic protocells) and bare magnetite nanoparticles against (a) U87 and (b) MCF7 cells after 72 hours of incubation. Bars marked with identical symbols indicating statistically significant differences when comparing together.

DOX IC50 indicates that the concentration of DOX required to inhibit the growth of 50% of cells in the given period [37]. The IC50 was calculated from the dose dependent cytotoxicity curves in the given period based on the equation $y = f(x)$ where y=50% and $f(x)$ is the fitted polynomial trend-lines for each curve. Therapeutic potential of the DOX loaded nanoparticles were evaluated by incubating cells with free DOX or DOX loaded nanoparticle solution with an equivalent amount of DOX (4.31, 8.62, 12.93 and 17.24 μM) for up to 72 hours. DOX IC50 against MCF7 and U87 cell lines both in free form and encapsulated are presented in

Table 1. Encapsulated DOX induced cytotoxicity was observed to be lower than free DOX. However it is reported in the literature that drug loaded mesoporous nanoparticles have higher cytotoxicity than free DOX against drug resistant cells [33, 38, 39]. The lower toxicity of encapsulated DOX could be attributed to the delayed drug release from nanoparticles and also different drug transport pathways into the cells. Free DOX molecules would transpor into the cells *via* passive diffusion mechanism while DOX loaded nanoparticles would enter the cells by endocytosis mechanism followed by a slow release of DOX molecules inside the cell [40, 41].

Table 1. Calculated IC50 of DOX against MCF7 and U87 cell lines

Exposure time	MCF7			U87		
	Free dox	Uncapped-DOX loaded Mesoporous nanocomposites	DOX loaded protocells	Free dox	Uncapped-DOX loaded Mesoporous nanocomposites	DOX loaded protocells
24 hours	6.68	>17.24	>17.24	11.39	>17.24	>17.24
48 hours	2.56	4.58	4.77	2.94	4.94	3.48
72 hours	1.87	2.53	2.44	2.02	2.65	2.69

Cytotoxicity test under AMF

Hyperthermia treatments in combination with radiotherapy, surgery or chemotherapy have proven to enhance treatment response and survival rates [42-45]. Magnetic hyperthermia is based on the localized heat generated by placing superparamagnetic iron oxide nanoparticles in an alternating magnetic field (AMF) to kill tumour cells. Cells were placed in an AMF for 45 minutes and the temperature was maintained at 43^{o} C by changing the magnetic field strength. The cells viability after magnetic hyperthermia treatment was measured upon 2 hours and 24 hours post treatment using the PrestoBlue viability assay. A group of control cells were placed in a water bath at 43°C for 45 mins and the cell viability was assessed to compare the effect of traditional heating and magnetic hyperthermia treatments. Another control group without magnetic nanoparticles were exposed to magnetic field for 45 minutes which didn't show any changes in cell viability indicating that magnetic field exposure doesn't cause any damage to the cells. The results are illustrated in Figure 6 andFigure 7 where it indicates that neither magnetic nanoparticles without the magnetic field nor magnetic field alone affected the viability of the cells.

The viability assay for magnetic hyperthermia compared with water bath heating performed 2 hours after the treatment established that both methods resulted in decreased cell viability. However a viability assay performed 24 hours post hyperthermia treatment indicated that cells incubated with protocells and exposed to magnetic hyperthermia continued to decay even after the AMF exposre. Cell viability was further reduced from 83.2% in 2 hours to 62.5% after 24 hours, for MCF7 cells and similarly from 91.1% to 66.2% for U87 cells. Continuous decline in cell viability

following magnetic hyperthermia may be as a result of cytoskeletal damage of the cells and initiation of apoptosis during the magnetic hyperthermia treatment. Balasubramanian *et al.* [46] have reported morphology changes of the cancer cells exposed to an AMF field with disintegrated actin filaments and shrunken morphology. The morphology change is considered as a sign of initiation of cell apoptosis.

Viability assays performed for cells incubated with DOX-loaded nanoparticles showed an increase in cell death both for water bath heating and magnetic hyperthermia heating at 43^0C compared to cells incubated at body temperature. However, the cell viability measured 2 hours after hyperthermia treatments with DOX loaded nanoparticles showed higher survival rates than cells treated with free DOX.

The cell viability measured 24 hours after magnetic hyperthermia treatment under AMF with DOX loaded nanoparticles showed further decrease in viable cells. The viability of MCF7 cells was reduced from 59.2% to 24.4% which is lower than free DOX in the same period (see Fig. 7). The cell viability for U87 measured 24 hours after magnetic hyperthermia treatment under AMF was decreased from 46.8% to 22.7% which is also lower than free DOX and water bath heat treated cells. The increased cell death after hyperthermia treatment with DOX loaded protocells could be the result of a combination of heat generated by the magnetic nanoparticles and enough concentration of drug molecules released inside the cell at that temperature. This has already been pointed in our abstract that the effect of pure DOX on cytotoxicity is lower compared to DOX loaded magnetic protocell under AMF. Furthermore, it has been reported [46] that the hyperthermia induce damage to the cell structure resulting in apoptosis.

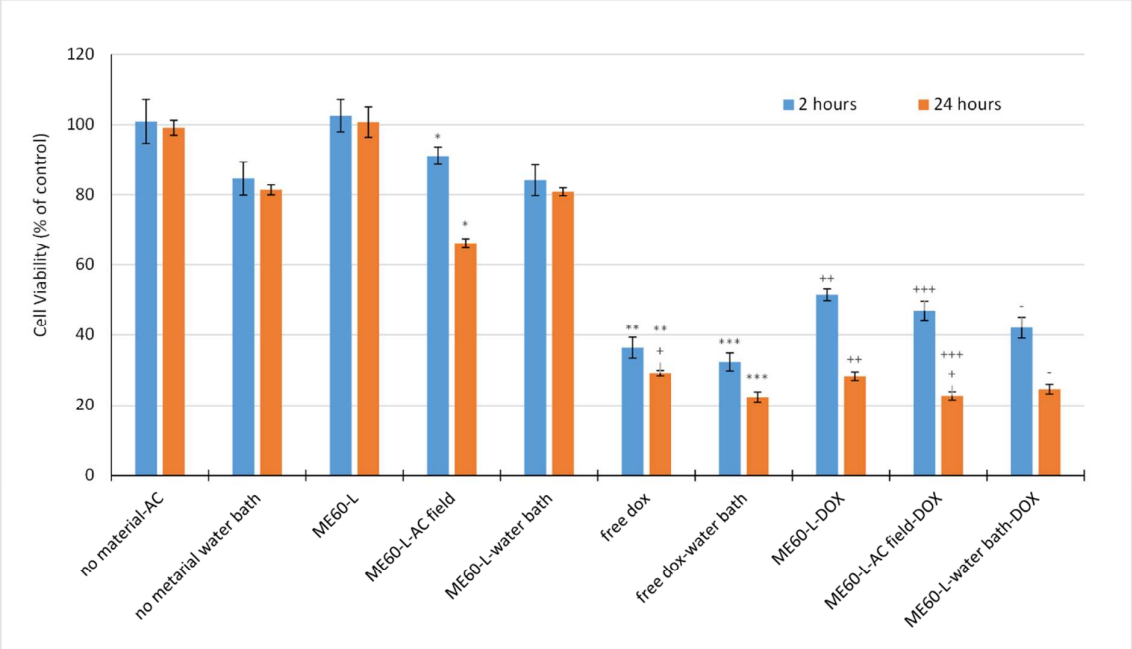

Figure 6. Effects of hyperthermia on U87 cells viability, The viability of cells incubated with protocells with (DOX concentration 17.24 μM) and without DOX and exposed to the magnetic field were compared to water bath hyperthermia treated cells (45 minutes treatment). ME60-L is representing protocell. Bars marked with identical symbols indicating statistically significant differences when comparing together.

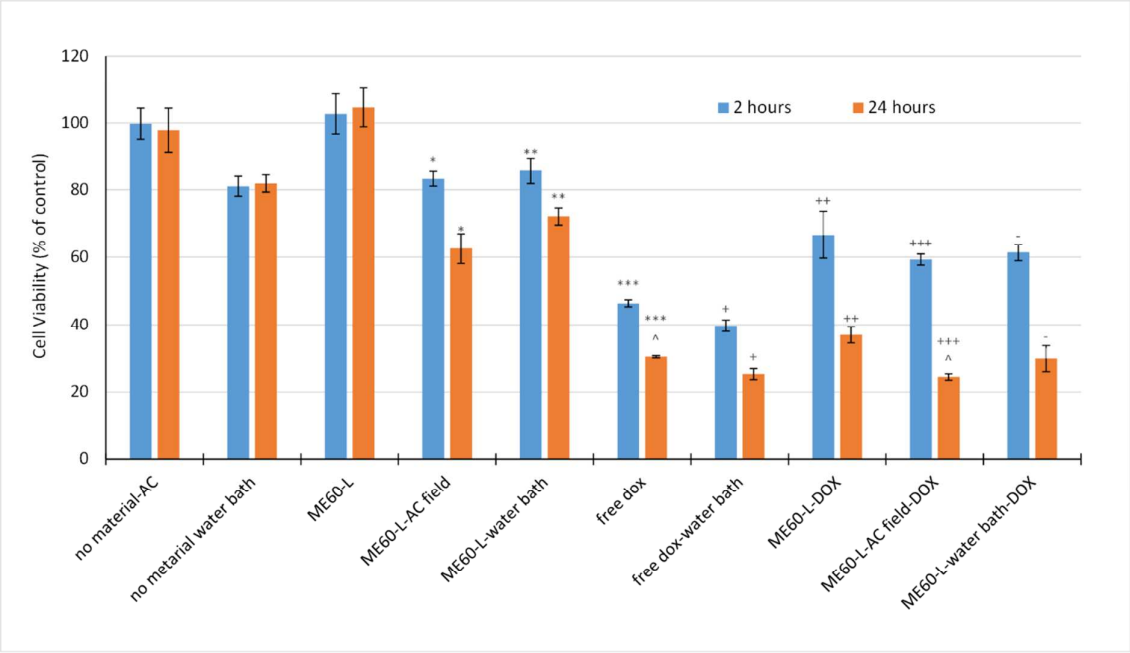

Figure 7. Effects of hyperthermia on MCF7 cells viability, The viability of cells incubated with protocells with (concentration of DOX: 17.24 μM) and without drug and exposed to AMF were compared to water bath heat

treated cells (45 minutes treatment). ME60-L is representing protocells. Bars marked with identical symbols indicating statistically significant differences when comparing together.

Conclusion & Future perspective

A novel liposome capped mesoporous silica coated magnetic nanoparticles "magnetic protocells" were efficient in loading DOX and exhibited a slow release under AMF at 43^{o} C. It was observed that the protocells were non-toxic to commercial cancer cell lines (U87 and MCF7) however DOX loaded protocells were efficient to kill the cells due to sufficient release of drugs and generating heat under AMF. DOX loaded protocells showed great potential for dual application (a) drug encapsulation/release (b) magnetic heating of the target cancer cells for future cancer therapy.

Financial & competing interest disclosure

This work has partly been supported by the UK India Education and Research Initiative (UKIERI) with the contract number DST/INT/UK/P-82/2014 as a part of project dissemination activity and partly by the Royal Society, UK by providing a small research grant (2014) for purchasing the Magnetic Hyperthermia equipment (DM100 series, Nanoscale Biomagnetics SL., Spain). The authors have no relevant affiliations or financial involvement with any organisation or entity with a financial interest in or financial conflict with the subject matter or materials discussed in the manuscript apart from those disclosed.

Ethical conduct of research

The authors state that they have obtained appropriate institutional review board approval.

Executive Summary

- In this article a novel nanomaterials "magnetic protocells" have developed via liposome capping of mesoporous silica coated magnetite nanoparticles

- Magnetic protocells are biocompatible against commercial cancer cell lines U87 and MCF87 however cell death has been observed upon heating under Alternating Magnetic Field (AMF)
- Magnetic protocells are efficient in anticancer drug (Doxorubicin) loading at 18^{o} C and releasing under AMF at 43^{o} C
- Drug loaded magnetic protocells had a dramatic effect on cell viability of U87 and MCF87 cell lines under AMF due to heating and drug release as dual treatment.
- This materials could be potential for targeted drug delivery under AMF in addition to hyperthermia heating treatment for future cancer therapy.

1. Siegel R, DeSantis C, Virgo K *et al*. Canccer treatment and survivorship statistics, 2012. *Cancer J. Clin.* 376(1), 67-75 (2012).
2. Wu X, Wang Z, Zhu D*, et al.* pH and Thermo Dual-Stimuli-Responsive Drug Carrier Based on Mesoporous Silica Nanoparticles Encapsulated in a Copolymer–Lipid Bilayer*. ACS Appl. Mater. Interfaces* 5(21), 10895-10903 (2013).
3. Mornet S, Vasseur S, Grasset F,Duguet E. Magnetic nanoparticle design for medical diagnosis and therapy. *J. Mater. Chem.* 14(14), 2161-2175 (2004).
4. Di Corato R, Espinosa A, Lartigue L*, et al.* Magnetic hyperthermia efficiency in the cellular environment for different nanoparticle designs*. Biomaterials* 35(24), 6400-6411 (2014).
5. Lu J, Liong M, Zink JI,Tamanoi F. Mesoporous Silica Nanoparticles as a Delivery System for Hydrophobic Anticancer Drugs*. Small* 3(8), 1341-1346 (2007).
6. Vogt C, Toprak M, Muhammed M, Laurent S, Bridot J-L,Müller R. High quality and tuneable silica shell–magnetic core nanoparticles. *J. Nanopart. Res.* 12(4), 1137-1147 (2010).
7. Slowing II, Trewyn BG,Lin VSY. Mesoporous Silica Nanoparticles for Intracellular Delivery of Membrane-Impermeable Proteins*. J. Am.Chem.Soc.* 129(28), 8845-8849 (2007).
8. Vallet-Regi M, Rámila A, Del Real RP,Pérez-Pariente J. A New Property of MCM-41: Drug Delivery System*. Chem. Mat.* 13(2), 308-311 (2001).
9. Mal NK, Fujiwara M, Tanaka Y. Photocontrolled reversible release of guest molecues from coumarin-modied mesoporous silica. *Nature* 421 (6921), 350-353 (2003).
10. Yang Y, Song W, Wang A, Zhu P, Fei J,Li J. Lipid coated mesoporous silica nanoparticles as photosensitive drug carriers*. Phys. Chem.Chem.Phys.* 12(17), 4418-4422 (2010).
11. Lingjie W, Ming W, Yongyi Z*, et al.* Multifunctional PEG modified DOX loaded mesoporous silica nanoparticle@CuS nanohybrids as photo-thermal agent and thermal-triggered drug release vehicle for hepatocellular carcinoma treatment*. Nanotechnology* 26(2), 025102 (2015).

12. Sahoo B, Devi KS, Dutta S, Maiti TK, Pramanik P,Dhara D. Biocompatible mesoporous silica-coated superparamagnetic manganese ferrite nanoparticles for targeted drug delivery and MR imaging applications. *J Colloid Interface Sci* 431 31-41 (2014).
13. Meng H, Mai WX, Zhang H, *et al.* Co-delivery of an Optimal Drug/siRNA Combination Using Mesoporous Silica Nanoparticle to Overcome Drug Resistance in Breast Cancer In Vitro and In Vivo. *ACS nano* 7(2), 994-1005 (2013).
14. Rosenholm JM, Sahlgren C,Linden M. Towards multifunctional, targeted drug delivery systems using mesoporous silica nanoparticles--opportunities & challenges. *Nanoscale* 2(10), 1870-1883 (2010).
15. Nakamura T, Sugihara F, Matsushita H, Yoshioka Y, Mizukami S,Kikuchi K. Mesoporous silica nanoparticles for 19F magnetic resonance imaging, fluorescence imaging, and drug delivery. *Chem. Sci.* 6(3), 1986-1990 (2015).
16. Rosenholm JM, Zhang J, Sun W,Gu H. Large-pore mesoporous silica-coated magnetite core-shell nanocomposites and their relevance for biomedical applications. *Microporous Mesoporous Mater.* 145(1-3), 14-20 (2011).
17. Lu J, Liong M, Li Z, Zink JI,Tamanoi F. Biocompatibility, Biodistribution, and Drug-Delivery Efficiency of Mesoporous Silica Nanoparticles for Cancer Therapy in Animals. *Small* 6(16), 1794-1805 (2010).
18. Liu J, Stace-Naughton A, Jiang X,Brinker CJ. Porous Nanoparticle Supported Lipid Bilayers (Protocells) as Delivery Vehicles. *J. Am.Chem.Soc.* 131(4), 1354-1355 (2009).
19. Wang L-S, Wu L-C, Lu S-Y, *et al.* Biofunctionalized Phospholipid-Capped Mesoporous Silica Nanoshuttles for Targeted Drug Delivery: Improved Water Suspensibility and Decreased Nonspecific Protein Binding. *ACS nano* 4(8), 4371-4379 (2010).
20. Li J, Wang X, Zhang T, *et al.* A review on phospholipids and their main applications in drug delivery systems. *Asian Journal of Pharmaceutical Sciences* 10(2), 81-98 (2015).
21. Ashley CE, Carnes EC, Phillips GK, *et al.* The targeted delivery of multicomponent cargos to cancer cells by nanoporous particle-supported lipid bilayers. *Nat Mater* 10(5), 389-397 (2011).
22. Podaru G, Ogden S, Baxter A, *et al.* Pulsed Magnetic Field Induced Fast Drug Release from Magneto Liposomes via Ultrasound Generation. *J. Phys. Chem. B* 118(40), 11715-11722 (2014).
23. Drummond DC, Meyer O, Hong K, Kirpotin DB,Papahadjopoulos D. Optimizing liposomes for delivery of chemotherapeutic agents to solid tumors. *Pharmacol. Rev.* 51(4), 691-743 (1999).
24. Sharifabad ME, Hodgson B, Jellite M, Mercer T,Sen T. Enzyme immobilised novel core-shell superparamagnetic nanocomposites for enantioselective formation of 4-(R)-hydroxycyclopent-2-en-1-(S)-acetate. *Chem. Commun.* 50(76), 11185-11187 (2014).
25. Sharifabad ME, Mercer T,Sen T. The fabrication and characterization of stable core-shell superparamagnetic nanocomposites for potential application in drug delivery. *J. Appl. Phys.* 117(17), 17D139 (2015).
26. Sen T, Sheppard SJ, Mercer T, Eizadi-Sharifabad M, Mahmoudi M,Elhissi A. Simple one-pot fabrication of ultra-stable core-shell superparamagnetic nanoparticles for potential application in drug delivery. *RSC Adv.* 2(12), 5221-5228 (2012).
27. Bañobre-López M, Teijeiro A,Rivas J. Magnetic nanoparticle-based hyperthermia for cancer treatment. *Rep. Prac. Oncol. Radiother.* 18(6), 397-400 (2013).
28. Kobayashi T. Cancer hyperthermia using magnetic nanoparticles. *Biotechnol. J.* 6(11), 1342-1347 (2011).
29. (Atcc) ATCC. MCF7 ATCC Â® HTB-22 Homo sapiens mammary gland, breast; deri. (2015).
30. (Atcc) ATCC. U-87 MG ATCC Â® HTB-14â„¢ Homo sapiens brain glioblastoma; astr. (2016).
31. Mahmoudi M, Sant S, Wang B, Laurent S,Sen T. Superparamagnetic iron oxide nanoparticles (SPIONs): Development, surface modification and applications in chemotherapy. *Adv. Drug Deliver. Rev.* 63(1-2), 24-46 (2011).
32. Mercer T,Bissell PR. The Observed Linearity and Detection Response of Magnetic Fluid Concentration Magnetometry - A Theoretical and Experimental Description. *IEEE Trans. Magn.* 49(7), 3516-3519 (2013).
33. Wang X, Teng Z, Wang H, *et al.* Increasing the cytotoxicity of doxorubicin in breast cancer MCF-7 cells with multidrug resistance using a mesoporous silica nanoparticle drug delivery system. *Int. J. Clin. Exp. Pathol.* 7(4), 1337-1347 (2014).
34. Yildirim A, Demirel GB, Erdem R, Senturk B, Tekinay T,Bayindir M. Pluronic polymer capped biocompatible mesoporous silica nanocarriers. *Chem. Commun.* 49(84), 9782-9784 (2013).

35. Xie M, Xu Y, Shen H, Shen S, Ge Y,Xie J. Negative-charge-functionalized mesoporous silica nanoparticles as drug vehicles targeting hepatocellular carcinoma. *Int. J. Pharm.* 474(1-2), 223-231 (2014).
36. Yu T, Malugin A,Ghandehari H. Impact of Silica Nanoparticle Design on Cellular Toxicity and Hemolytic Activity. *ACS nano* 5(7), 5717-5728 (2011).
37. Osman A-MM, Bayoumi HM, Al-Harthi SE, Damanhouri ZA,Elshal MF. Modulation of doxorubicin cytotoxicity by resveratrol in a human breast cancer cell line. *Cancer. Cell. Int.* 12(1), 47 (2012).
38. Huang IP, Sun SP, Cheng SH, *et al.* Enhanced chemotherapy of cancer using pH-sensitive mesoporous silica nanoparticles to antagonize P-glycoprotein-mediated drug resistance. *Mol. Can. Ther.* 10(5), 761-769 (2011).
39. Shen J, He Q, Gao Y, Shi J,Li Y. Mesoporous silica nanoparticles loading doxorubicin reverse multidrug resistance: performance and mechanism. *Nanoscale* 3(10), 4314-4322 (2011).
40. Gai S, Yang P, Ma PA, *et al.* Fibrous-structured magnetic and mesoporous Fe3O4/silica microspheres: synthesis and intracellular doxorubicin delivery. *J. Mater.Chem.* 21(41), 16420-16426 (2011).
41. Kim J, Kim HS, Lee N, *et al.* Multifunctional uniform nanoparticles composed of a magnetite nanocrystal core and a mesoporous silica shell for magnetic resonance and fluorescence imaging and for drug delivery. *Angew. Chem. Int. Ed. (English).* 47(44), 8438-8441 (2008).
42. Johannsen M, Gneveckow U, Eckelt L, *et al.* Clinical hyperthermia of prostate cancer using magnetic nanoparticles: Presentation of a new interstitial technique. *Int. J. Hyperthe.* 21(7), 637-647 (2005).
43. Maier-Hauff K, Ulrich F, Nestler D, *et al.* Efficacy and safety of intratumoral thermotherapy using magnetic iron-oxide nanoparticles combined with external beam radiotherapy on patients with recurrent glioblastoma multiforme. *J. Neurooncol.* 103(2), 317-324 (2011).
44. Sadhukha T, Niu L, Wiedmann TS,Panyam J. Effective Elimination of Cancer Stem Cells by Magnetic Hyperthermia. *Mol. Pharm.* 10(4), 1432-1441 (2013).
45. Asín L, Ibarra MR, Tres A,Goya GF. Controlled Cell Death by Magnetic Hyperthermia: Effects of Exposure Time, Field Amplitude, and Nanoparticle Concentration. *Pharm. Res.* 29(5), 1319-1327 (2012).
46. Balasubramanian S, Girija AR, Nagaoka Y, *et al.* Curcumin and 5-Fluorouracil-loaded, folate- and transferrin-decorated polymeric magnetic nanoformulation: a synergistic cancer therapeutic approach, accelerated by magnetic hyperthermia. *Int. J. Nanomedicine.* 9 437-459 (2014).